

Review

3D Numerical Modeling of Geosynthetics for Soil Reinforcement: A Bibliometric Analysis and Literature Review

Lucas Paiva ¹, Margarida Pinho-Lopes ^{1,*}, António Miguel Paula ² and Robertt Valente ³

- ¹ Research Center for Risks and Sustainability in Construction, Department of Civil Engineering, University of Aveiro, Campus Universitário de Santiago, 3810-193 Aveiro, Portugal; lucaspaiva@ua.pt
- ² Instituto Politécnico de Bragança, Campus de Santa Apolónia, 5300-253 Bragança, Portugal; mpaula@ipb.pt
- ³ Centre for Mechanical Technology and Automation, Department of Mechanical Engineering, University of Aveiro, Campus Universitário de Santiago, 3810-193 Aveiro, Portugal; robertt@ua.pt
- * Correspondence: mlopes@ua.pt

Abstract: Soil reinforcement using geosynthetics is an efficient and cost-effective solution for a variety of geotechnical structures. Along with the increasing use of geosynthetics, there is a need to expand and enhance the design methodologies for these elements, which are still frequently based on conservative limit equilibrium approaches. In this paper, a bibliometric analysis was conducted on geosynthetic-reinforced soil structures (GRS), identifying the state of the art, research trends, and other indicators. The data were obtained from the Scopus platform and processed by VOSViewer v1.6 software. The initial search comprised 552 papers and the screening process selected 516 relevant papers from 1992 to October 2023. The study analyzed the occurrence of publications by year, keyword trends, authors, citations/co-citations, and bibliographic coupling. Then, a focus was given to 3D modeling research on geosynthetics, highlighting the dominant modeling techniques, material properties, and design challenges in GRS. The bibliometric analysis provided a crucial guideline in the identification of relevant papers and research trends, and a series of conclusions were presented regarding the 3D modeling techniques, choice of material properties, and boundary conditions.

Keywords: geotechnical engineering; geosynthetics; soil-geosynthetic; numerical modelling; 3D modelling; bibliometric analysis



Citation: Paiva, L.; Pinho-Lopes, M.; Paula, A.M.; Valente, R. 3D Numerical Modeling of Geosynthetics for Soil Reinforcement: A Bibliometric Analysis and Literature Review. *Geotechnics* **2024**, *4*, 673–692. <https://doi.org/10.3390/geotechnics4020036>

Academic Editor: Raffaele Di Laora

Received: 14 May 2024
Revised: 5 June 2024
Accepted: 12 June 2024
Published: 18 June 2024



Copyright: © 2024 by the authors. Licensee MDPI, Basel, Switzerland. This article is an open access article distributed under the terms and conditions of the Creative Commons Attribution (CC BY) license (<https://creativecommons.org/licenses/by/4.0/>).

1. Introduction

Geotechnical structures are a key component of almost all infrastructure projects and are therefore of utmost importance to the economy of any country. Geosynthetics are known to be an efficient and cost-effective solution for many geotechnical structures. Geosynthetics are manufactured polymeric materials used with soil, rock, and other earth-related materials as an integral part of a project or system. Reinforcements are used to produce a soil–geosynthetic composite that has improved strength and deformation properties over unreinforced soil. There are many applications (e.g., transportation, environmental, hydraulics) where geosynthetics are used as reinforcement [1], with economic, performance, and environmental advantages. The design and analysis of structures with geosynthetic-reinforced soil are often carried out using numerical simulations, an approach that nevertheless presents unique challenges. The use of methodologies based on modeling and numerical simulation is grounded in the fact that the conventional design of geosynthetic structures is commonly conservative. For example, one study [2] showed that the analytic design of geosynthetic-reinforced soil walls using the North American standard was extremely conservative, underestimating the geosynthetic performance by 50%. A more recent comparison [3] of analytical methods provided by technical standards also showed considerable overestimation of the loads acting on the reinforcement.

There are many recurring difficulties in geosynthetic-reinforced soil (GRS) modeling as reported by the literature. Large deformations in unreinforced and reinforced geotechnical

structures can occur in soft soils and, in these cases, the finite element method (FEM) can prove somewhat limited due to mesh distortion issues [4,5]. Mesh distortion arises when the elements of the computed mesh become excessively deformed under the presence of large deformations. This distortion leads to several problems. Firstly, the quality of the elements degrades, as elements that are initially well-shaped become skewed or stretched, reducing the accuracy of the model representation. Secondly, distorted elements can cause numerical instability, making the stiffness matrix poorly conditioned and leading to significant errors in the results, because the integration points and finite element shape functions may no longer be appropriately distributed.

Due to the relatively scarce amount of reported large-scale controlled and properly instrumented GRS structures, many numerical modeling attempts are validated with simple limit equilibrium methods, which can lead to a conservative estimation of the forces acting on the reinforcement [6,7]. Even fewer studies, e.g., [8–10], have proposed a FEM model that was directly compared to experimentally measured data of soil and reinforcement, and there are often disparities in magnitude and tendencies between the predicted and measured values.

Since the construction and monitoring of large-scale and full-scale GRS structures are expensive and time-consuming, reduced-scale experiments have been proposed to analyze the stress distribution within the reinforcement. In [11], the authors showcased that there are discrepancies when evaluating the stress concentrations and their distributions on reduced-scale structures in comparison with full-scale experimental data from the literature. There are several causes for such discrepancies. For example, the stress level on small-scale models is significantly lower than in full-scale structures. Moreover, their study pointed out several cases where the standards grossly underestimated the stress concentration ratio on the reduced-scale models. This indicates that a high level of non-linearity can be a determining factor in the scalability of a model.

One of the most important aspects of the design of geotechnical structures for both reinforced and unreinforced soils is the selection of failure criteria and the corresponding constitutive models. This applies to both soils and reinforcements. The tensile response of geosynthetics is nonlinear for both the short- and long-term, hence corresponding nonlinear models should be applied to better represent the behavior of these elements [12]. Geosynthetics can be defined by physical or numerical models, whether there is a correlation between the model parameters and the material properties (physical) or not (numerical). Physical models are of particular interest, since they are derived from equations that can be correlated with material properties. A common modeling approach is to define a linear stiffness from standardized in-isolation wide-width tensile tests, e.g., according to ISO-10319:2015 [13]. However, the true performance of a geosynthetic reinforcement under in situ operational conditions is unlikely to be reflected by an in-isolation rapid test [14]. Moreover, it is common to adopt simplifications of the geometry of the reinforcement, namely on geogrids and geonets. To reduce the model complexity when dealing with reinforcements that contain apertures, an equivalent 2D shell/membrane is sometimes adopted [15,16].

Geosynthetics are considered elasto-viscoplastic materials; their durability is another key feature of their design. Thus, realistic constitutive models for representing the response of geosynthetics should also allow for the effects of durability issues. For geosynthetic reinforcements, the design is often based on the short-term tensile strength affected by reduction factors that represent the effects of different degradation agents and mechanisms. In GRS structures, mechanical damage associated with field installation is a major aspect of durability. In addition, because of their time-dependent response, in design, it is common to affect the tensile strength of geosynthetics by a reduction factor representing the effect of creep. There are also additional reduction factors that can be applied if needed: seams and dynamic influences; as well as the influence of atmospheric, chemical, and biological agents can also be represented by reduction factors. Thus, current design methods apply reduction factors to the ultimate short-term tensile strength, by including relevant reduction factors

that represent the effect of a single agent or mechanism affecting the tensile strength of the reinforcement, which results in an allowable tensile strength. However, this approach is known to be conservative, since not only the admissible strength is affected by the combination of reduction factors, but also the serviceability and failure patterns [17,18].

This paper aims to provide a comprehensive literature review on the latest (2005–2023) three-dimensional (3D) GRS numerical modeling studies. The proposed review features relevant information on the following:

- Whether the available numerical models are backed by experimental data;
- The covered simulation goals of each referred approach (e.g., working conditions (SLS), predict ultimate limit state, (ULS), results or carry out parametric analysis);
- Relevant constitutive models for geosynthetic and soils;
- Consideration of soil–geosynthetic interaction.

2. Methodology

To better understand the state of the art of the 3D numerical modeling of GRS structures, a bibliometric analysis was conducted using the Scopus database and VOSviewer v.1.6.20 software. A bibliometric analysis is a method for identifying research trends and can be used to visualize how knowledge is established in a particular field [19]. This methodology has become popular in the past decade as the amount of information in various areas of science has rapidly grown, leading to a longer time spent in finding and compiling relevant literature. To this end, bibliometric analysis has proven to be an efficient method for searching and selecting relevant literature [20].

The Scopus platform was used to collect published papers with the following described criteria, divided into three steps. The query for the main terms that are the focus of this analysis, i.e., “geosynthetics, reinforcement, modeling”, led to more than 4000 results when the search was performed in October 2023. As many of the documents found in this first search were not directly related to the modeling of GRS structures, an advanced search was performed. One technique to filter sparse results in Scopus is to limit the keyword search to specific fields, i.e., keywords in the title or the abstract. The following criteria were adopted (Figure 1): keywords (geosynthetics, AND reinforcement, AND modelling) that appear in (paper title, OR abstract OR keywords). It should be noted that the Scopus search engine automatically includes the American spelling of keywords in the results. From this search, 552 papers were found. This result was better adjusted to the research goals of the present paper. A screening step was also included before the data analysis. In order to access the annual trends, the results were limited to articles in the final publication stage up to October 2023 and articles written in English. From this screening, 36 documents were excluded. Thus, 516 papers with seven main document types were selected for the analysis phase (Figure 1). The two most frequent document types were articles (75%) and conference papers (22%).

Step 1: Data collection	Step 2: Screening	Step 3: Bibliometric Analysis
Database: Scopus	Time frame: Up to Oct. 2023	Annual output and trends
Search mode: Advanced	Pub. stage: Final	Co-occurrence of keywords
Variables: Geosynthetics; Reinforcement; Modelling.	Language: English	
Search within: Title; Abstract; Keywords.	Final number of papers: 516	
Number of documents: 552		

Figure 1. Steps of the bibliometric analysis carried out in the present paper.

Two analysis types were used in this paper. The first analysis extracted the growth trends and other one-variable metrics from the comma-separated values obtained directly from the Scopus platform. It was possible to gather information related to the number of publications by year, document category, country of origin, and most frequent authors. This simplistic approach provides some hints regarding the research interest of a given topic and which papers and authors should be more deeply analyzed. The second analysis type was performed through the data visualization software VOSviewer. Characterizing the “bigger picture” in a scientific field is desirable for a variety of reasons. However, outdated brute force methods that require an unfeasible amount of time to perceive basic outlines in research trends are no longer an option [21]. A bibliometric analysis provides a fresh approach to the literature review task by using clustering techniques that can, for instance, highlight groups of related publications, authors or journals. Bibliometric maps are a graphical visualization of the relatedness of publications. A set of papers can be analyzed according to their citation relations or word relations. By further comparing the relatedness of multiple documents, VOSviewer can draw clusters that can guide a well-structured literature review [19].

3. Data Analysis

3.1. Metrics and Annual Trends

3.1.1. Publications by Year

The first article related to geosynthetics modeling in the database was from 1992 and it was published in the Journal of Geotextiles and Geomembranes, with the Title: “Arrhenius modelling to predict geosynthetic degradation” [22]. This paper provided a simplified approach to analyzing the time-dependency of many geosynthetic properties (including creep) using high-temperature incubation tests. Publications on the subject became more frequent in 2009 when 25 papers meeting the search criteria used were published. Figure 2 illustrates the annual trends in publications generated from the database between 1992 and 2023. The number of publications peaked in 2022 with 44 published articles.

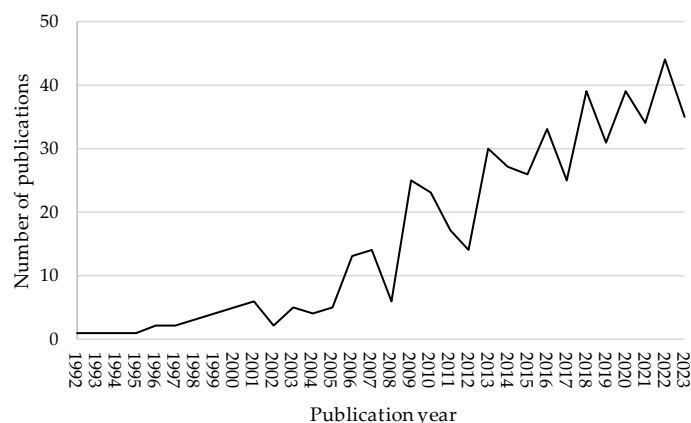


Figure 2. Annual trend in GRS publications meeting the search criteria.

3.1.2. Publications by Country

Analyzing the authors’ country of affiliation, it is possible to infer that this research field is of global interest, with 481 papers distributed across 53 countries; that is, at least one paper was published coming from these countries. Table 1 lists the top 10 countries that have produced the most publications in the area of interest, together accounting for 98% of all published papers.

Table 1. Number of publications meeting the search criteria described by author’s country of affiliation.

Rank	Country	Number of Papers	% of 516
1	United States of America	107	20.7%
2	India	79	15.3%
3	China	66	12.8%
4	Australia	43	8.3%
5	Canada	43	8.3%
6	Iran	38	7.4%
7	France	32	6.2%
8	Brazil	29	5.6%
9	United Kingdom	25	4.8%
10	Italy	19	3.7%

Figure 3 shows a map with the country of authorship from the database reported. It is possible to identify the main color clusters of India, the United States of America, Canada, and the United Kingdom. The colors indicate that the publications assigned to these countries are often related in terms of keyword frequency. The lines connecting the points on the map indicate the authorship between countries, and the distance between the clusters indicates the strength of cooperation. This map indicates where papers on GRS structures meeting the criteria used herein were researched the most.

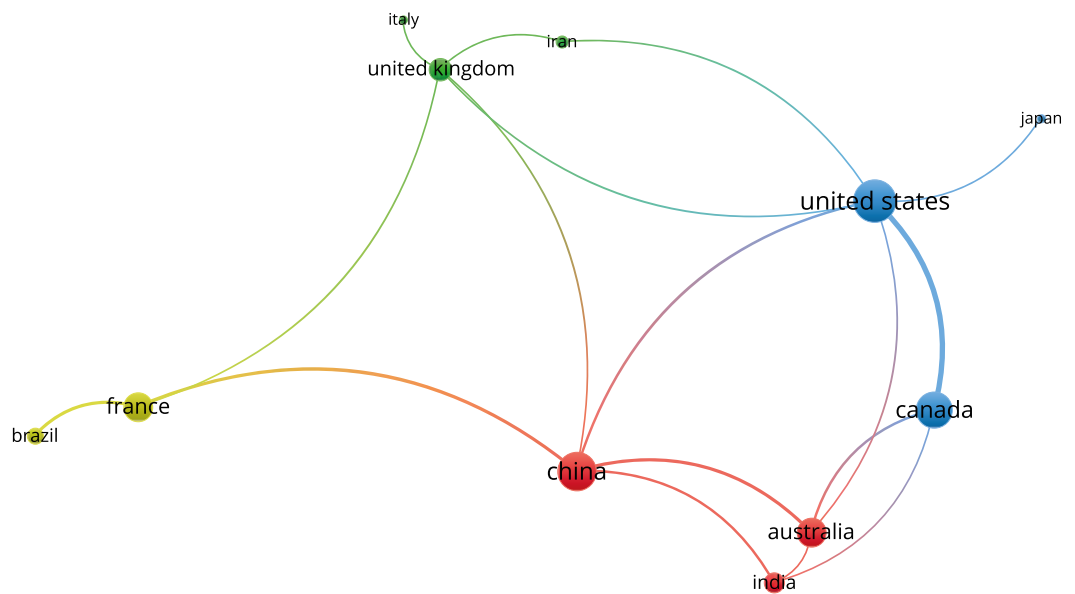


Figure 3. Co-authorship of countries for the papers meeting the search criteria.

3.1.3. Publications by Author

The last metric analysis addressed the production and publication by author. Table 2 identifies the top 10 most prolific authors. Professor Richard J. Bathurst from the Royal Military College of Canada is the author of 18 papers and accounts for 3.5% of the 516 papers analyzed, followed by Professor Jie Han from Kansas University, with 16 papers and a 3.1% share of the total publication sample strength.

Table 2. Top 10 most prolific authors of papers meeting the search criteria.

Country	Number of Papers	% of 516
Bathurst, R.J.	18	3.5%
Han, J.	16	3.1%
Viswanadham, B.V.S.	16	3.1%
Dias, D.	15	2.9%
Hatami, K.	13	2.5%
Ehrlich, M.	11	2.1%
Mirmoradi, S.H.	10	1.9%
Thorel, L.	10	1.9%
Zomberg, J.G.	10	1.9%
Briançon, L.	9	1.7%

3.2. Bibliometric Analysis

Co-Occurrence of Keywords

The co-occurrence map in Figure 4 illustrates the keyword relatedness (in this case, Authors’ and Indexes’ keywords) based on how frequently they occur in the paper. The nodes represent the keywords, and when they frequently appear together within a document, they form a cluster, illustrated with different colors (blue, green, and red in this case). In VOSViewer, clusters are non-overlapping and do not need to exhaustively cover all items in a map. Node colors are based on the frequency with which the keyword occurs in each publication. Keywords with greater frequency in more recent publications have a lighter color, compared to those frequently occurring in past publications.

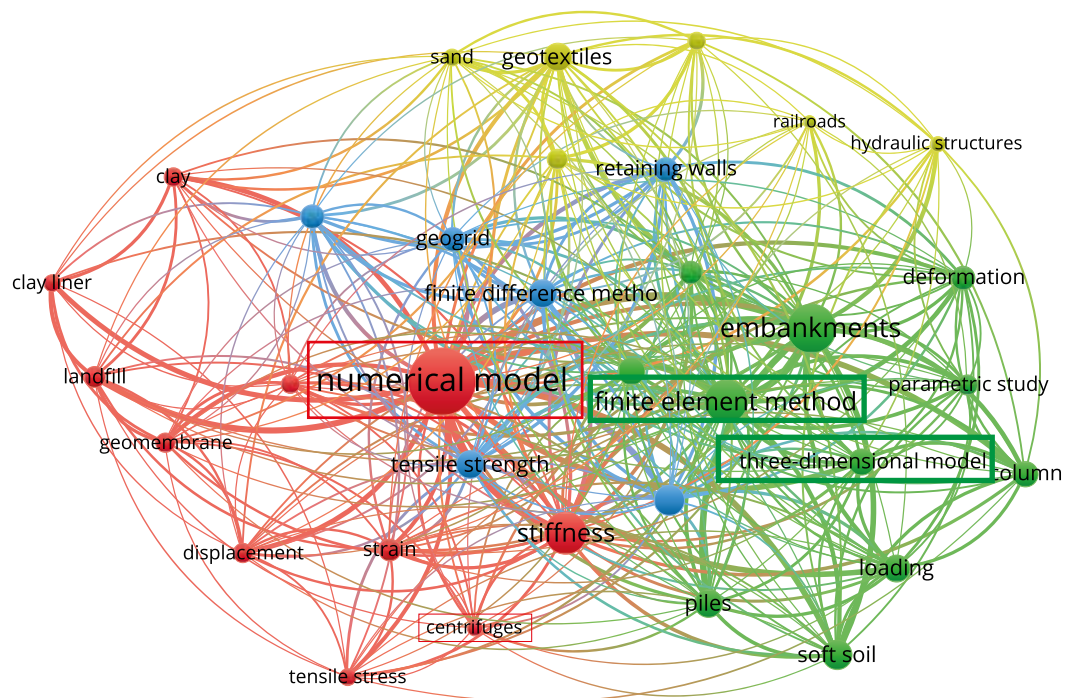


Figure 4. Co-occurrence of keywords map for papers meeting the search criteria.

VOSViewer can also generate an overlay visualization, Figure 5, where the shown parameter is the average publication year. Figure 5 indicates that, although numerical models were consistently applied, three-dimensional models were less common. In fact, from the 516 papers found related to the modeling of GRS structures, only 23 focused on 3D modeling, and the overlay map indicates that this is a more recent approach (average publication year: 2016).

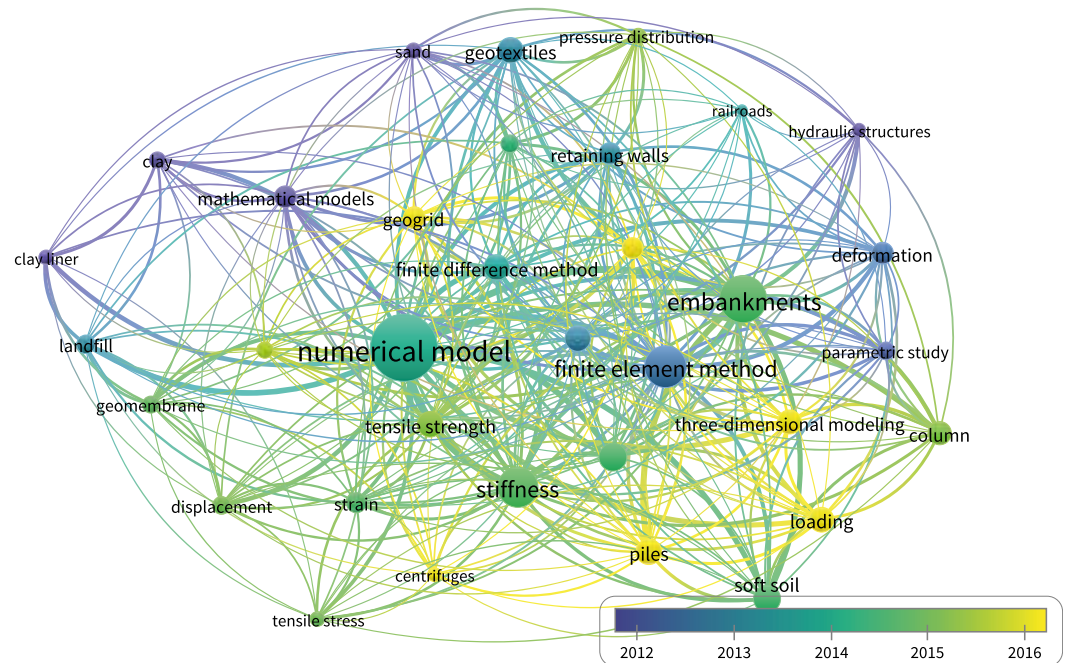


Figure 5. Average publication year of co-occurring keywords for papers meeting the search criteria.

The evolving field of geosynthetics research employs a plethora of methodologies and techniques to analyze complex soil–structure interactions. To identify key trends within this domain, the co-occurrence map generated using VOSViewer can be used to easily pinpoint central keywords and their interconnections. Although the primary focus of this review is on 3D modeling within geosynthetics—a topic explored in subsequent sections—it is crucial to acknowledge other significant avenues of research that contribute to a holistic understanding of the field.

In Figure 4, a noticeable “red cluster” emerged, anchored by the keyword “Numerical Model”. This term was frequently associated with other keywords such as “stiffness”, “finite element method”, and “soil–structure interaction”. This confluence of terms underlines the centrality of numerical models in geosynthetic research, serving as a basis for understanding the multifaceted nature of numerical modeling approaches, including 3D models.

The red in the co-occurrence map also draws attention to the utility of centrifuge modeling in the study of GRS structures. Unlike conventional full-scale tests, which are both time-consuming and expensive, centrifuge modeling offers an efficient alternative. By spinning a reduced-scale model in a higher gravitational field, the method emulates full-scale stresses and conditions. This technique is relatively novel in the context of reinforced soil, as the stress levels introduced by reinforcement are considerably higher than those found in non-reinforced soil [23]. A prime example of using centrifuge model results combined with numerical analysis was presented by [24]. This study carried out a 2D/3D numerical analysis of a geosynthetic-reinforced pile validated by a reduced-scale centrifuge test. The experimental test was composed of a 1/20 scaled pile reinforced with a woven biaxial geotextile, using a centrifugal acceleration equal to 20 times the standard Earth gravity acceleration. The numerical analysis used the FEM implemented in the commercial software PLAXIS v8. The soil was numerically represented by the hardening soil model and also a hypoplastic model. The geotextile was modeled by two isotropic models, i.e., a hyperbolic curve including the hardening effect and a hypoplastic model (both for representing the short-term response). While the numerical model did not consider creep and overestimated the arching effect, the comparison between the numerical and experimental results revealed a good agreement. The numerical analysis offered insights into load transfer and the progression of differential settlement, as well as the strain behavior of the geotextile. The occurrence of movement within the soil–geosynthetic layer

could be observed at any location within the numerical model, although the experimental data were only captured in the center portion of the centrifuge. After calibration, several parametric variations were investigated, i.e., the pile spacing and thickness of soil mattress (soil above the geotextile supported by the pile). The centrifuge model test provided a convenient apparatus to simulate a reduced-scale GRS under a parametric test, which is rarely a viable option in alternative experimental methods.

Beyond the finite element method, the co-occurrence map indicated the finite difference method (FDM) as another vital numerical approach, particularly suited for predicting the large strains often observed in GRS structures like landfills and embankments. In [25], the FDM was used to model a landfill lining, reinforced with a textured geomembrane and nonwoven geotextiles. The system was expected to produce large deformations (>100 mm) that could generate post-peak strengths and mobilize high tensile strains in the geomembrane/geotextile layers, the reason why the FDM approach was preferred. The geosynthetics were represented as linear-elastic beam elements, and the subgrade materials were modeled using the elastic perfectly-plastic Mohr-Coulomb model (EPPMC). Other authors have used the FDM, which proved to be a good alternative for overcoming mesh generation problems when facing large deformations, and also for complex geometries, such as staggered wall joints [26].

The landscape of geosynthetic research is diverse, with multiple numerical and experimental approaches. While this review focused on the 3D modeling subfield, acknowledging the roles, advantages, and limitations of other techniques like centrifuge modeling and FDM allows for a comprehensive grasp of the field, with these intersecting methodologies serving as tools for advancing the understanding of GRS structures.

4. Literature Review on 3D Modeling of GRS for Reinforcement

Between 2005 and 2023, 3D numerical modeling in GRS became increasingly significant for understanding soil–structure interactions and predicting the behavior of these systems. This chapter presents a comprehensive literature review on the topic, highlighting key aspects of the papers found in the bibliometric analysis performed. A brief description of each model is hereby presented, highlighting the validity of the numerical models, specifically whether they were supported by the experimental data. Additionally, the review examines the specific objectives of each study, from replicating actual working conditions to predicting ULS outcomes or conducting parametric analyses. A primary focus was given to the choice of constitutive models and numerical formulations for representing both geosynthetics and soil, given its importance in ensuring the accuracy of model predictions. Furthermore, this review evaluated the consideration given to the interactions between soil and geosynthetic materials, whenever such properties were defined.

Huang et al. [27] reported one of the first 3D modeling attempts to analyze the performance of embankments over soft soil using the Fast Lagrangian Analysis of Continua (FLAC[®]) 2.1 package. This model aimed to replicate the working conditions of a real embankment that was instrumented and monitored. The model included a 6-pile embankment, reinforced with three geogrid layers. The EPPMC model was used to represent the soil and fill materials. A custom type of shell element built in the FLAC[®] package was used to model the geogrid element, assuming an isotropic response. The soil–geogrid interface was not modeled. The simulation included the construction phases by adding the embankment fill-in layers. The model was able to predict settlement with reasonable accuracy, but predictions of horizontal displacements did not adjust the experimental data. The linear-elastic isotropic model used to represent the geogrid overestimated the distribution of tensile forces acting on the geogrid when compared to the measured data.

In reference [28], a study of geosynthetics in pavement foundations with the software Automatic Dynamic Incremental Nonlinear Analysis (ADINA[®]) is presented. A theoretical (not backed by experimental data) parametric study was carried out to optimize the reinforcement layer position within the pavement composition. Three-dimensional models are particularly useful for pavement analysis, accounting for the complex behavior of

the composite structure and allowing the simulation of the rectangular footprint of the loading wheel. The geogrid was layer assumed to act as a linear isotropic elastic material modeled by a membrane element with four nodes and only in-plane tension stresses. The granular base was modeled with a Drucker–Prager (elasto-plastic) envelope, and for the subgrade, the CamClay model (elasto-plastic) was used. The biggest limitation reported was regarding the pullout behavior due to shear stresses, since the model did not account for the slippage/friction between the material layers. The simulation showed that the optimal position of the reinforcement was conditioned to the base stiffness and thickness, with reductions in fatigue strains between 10% and 48%. Although the inclusion of a geogrid for this pavement foundation greatly improved the strain performance, large discrepancies were reported when comparing the fatigue strain reductions with similar results from the literature.

Hello and Villard [29] focused on the load transfer mechanisms of geosynthetic and pile-reinforced embankments with YADE[®] software. Their study featured a coupled FEM and discrete element method (DEM) approach that maximized the accuracy of the response by using finite elements for the structure and geotextile, but discrete elements to simulate the soil. FEM is broadly (and efficiently) used to model not only structural elements but also discrete elements such as soils. However, the discontinuous nature of the soil that interacts with a geogrid could be better explored with DEM elements, that perform well for soil analysis, but cannot fully capture the “continuous” structural components due to microvoids. The soil particles were modeled in YADE[®] according to Newton’s laws of motion, requiring the definition of the macro-mechanical parameters (granular distribution and porosity) and micro-mechanical parameters (friction angle, normal, and tangential rigidity). The geotextile was modeled using 3-node finite elements that captured the membrane behavior of tensile strength with no rigidity to bending. Contact laws between particles governed how these two types of components interacted. The micro-mechanical parameters needed to characterize the geosynthetic sheet and its interaction with discrete particles were a normal and tangential rigidity of contact and a friction angle between the geotextile and soil. A parametric study was carried out to evaluate the two main mechanisms of piles, i.e., the arching effect and the membrane effect of the geotextile. The model was also compared against analytical and experimental results. The coupled FEM–DEM analysis was able to successfully represent the arching effect and membrane resistance (Figure 6) of piles reinforced with geotextiles. The vertical displacements obtained by the numerical model were very close to the experimental results, while the load measured on the piles was slightly higher for the simulation [29].

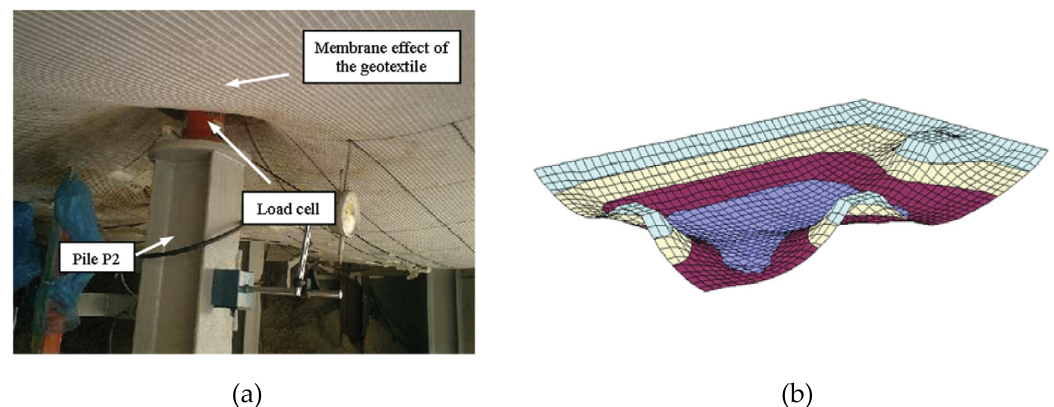


Figure 6. (a) Observed membrane effect on experimental test; (b) Simulation of membrane effect on geotextile [29].

A numerical investigation of the performance of geosynthetic-encased stone columns (GESC) for an embankment was presented in [30]. The study featured a real GESC embankment to calibrate the numerical model (cross-section Figure 7, then a parametric analysis

was conducted to evaluate the influence of mechanical properties (consistency of soft ground, stiffness of geosynthetic) and geometrical properties (length of encasement, area replacement ratio) on the obtained results. Soil elements, such as clay, stone, and fill, were modeled in ABAQUS[®] with twenty node pore-pressure elements (designated C3D20RP) using a modified CamClay model (for the clay) and the EPPMC model (stone and fill). The geosynthetic was represented by an 8-node membrane element (designated M3D8R) as a linear-elastic material without bending stiffness. No pore-pressure was assumed to develop between interfaces; thus, no interaction/interface laws were defined. The parametric study demonstrated the impact of the geosynthetic stiffness on the development of the pore pressure, which could be related to the embankment load transfer mechanism (stiffer geosynthetics decreased deformations and increased load bearing). Lateral bulging was also considerably decreased due to confinement by the encasement. The parametric data also suggested that the benefit of a stiffer geosynthetic reached a limit value (for this case, between approximately 1500 and 2000 kN/m), at which no meaningful resistance was added for further increases in stiffness.

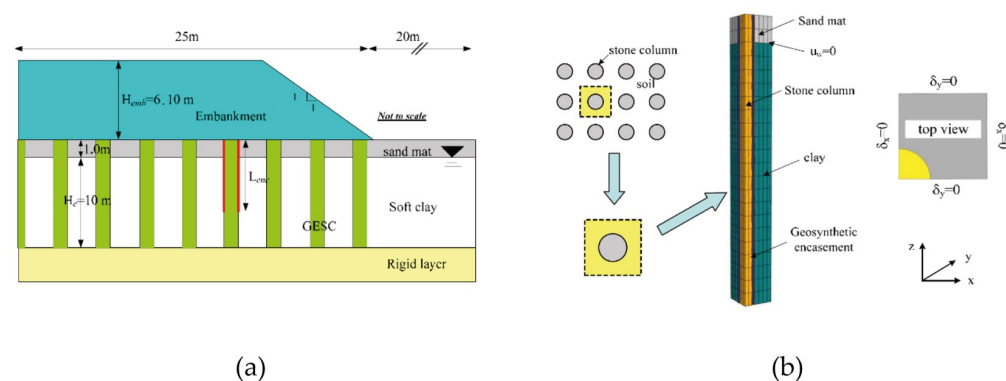


Figure 7. (a) Cross-section of GESC model; (b) 3D column model [30].

A comprehensive 3D FEM analysis of four different embankment solutions validated by field data was reported by [31]. Four instrumented sections were constructed: (i) an embankment without piles or reinforcement, (ii) an unreinforced pile-supported embankment, (iii) an embankment with pile-support and a geotextile layer reinforced gravel platform, and (iv) an embankment with pile-support and a two-layer geogrid reinforced gravel platform. A 3D representative slice of each of the four embankments was modeled in ABAQUS[®]. Piles, embankment fill, and soil above water were modeled with 20-node brick elements (designated C3D20R) and an EPPMC model. The soil below the water was modeled with 20-node brick elements, allowing for the pore pressure parameter (designated C3D20RP). Geosynthetics were represented by membrane elements without bending resistance (designated M3D8R), assuming a linear-elastic regime. Interface elements between pile/soil, embankment-fill/reinforcement, and embankment/subsoil were defined by a master/slave contact with basic Coulomb friction. Settlements were accurately predicted by the model during the whole construction phase, overestimating the settlement by an average of 8%, but the simulated settlement for the end of construction did not adjust the field data. The authors pointed out that changes in hydraulic conductivity and void ratio that were not considered in the model were likely the main reason for the deviation in the prediction. The strains acting on the reinforcement layer were in good agreement with the field data, which could also correctly predict the minimum and maximum strain locations in the reinforcement.

Tran et al. [32] used YADE software to analyze the soil–geosynthetic interaction of a geogrid-reinforced strip footing. The soil was defined as discrete elements with classic formulations (Newton’s and Euler’s equations). The biaxial geogrid was modeled as linear-elastic using 8-node brick elements (FE). An illustration of the FE/DE combination is shown

in Figure 8. Although 3D, the geogrid geometry did not include the different thicknesses of ribs and junctions. Interface elements (FE) with a tangential friction angle coefficient were also used to represent the soil–geogrid interaction. According to the authors, this coefficient had to be determined by trial and error. A multiple time-step approach was also required, since FE's time steps are much larger than DE's time steps. The procedural steps involved in a typical cycle of calculations can be succinctly summarized as follows: The first step involves determining the potential interactions between discrete element (DE) particles and the interactions between DEs and interface elements. Following this, the contact parameters for each interaction are determined using the appropriate contact laws. Subsequently, the interaction forces between DE particles and between DEs and interface elements are calculated. Finally, the velocities and positions of the particles are determined. The finite element (FE) solver is executed at regular intervals of n time steps, during which the forces acting on the FE nodes are updated to determine the displacements of the nodes. The coupled model was compared to experimental data and showed very good agreement in predicting failure modes and well adjusted the overall soil-reinforcement response. Parametric studies regarding the geogrid position and number of layers, with the simulation of erosion and the inclusion of soil voids, were also reported to agree with literature results.

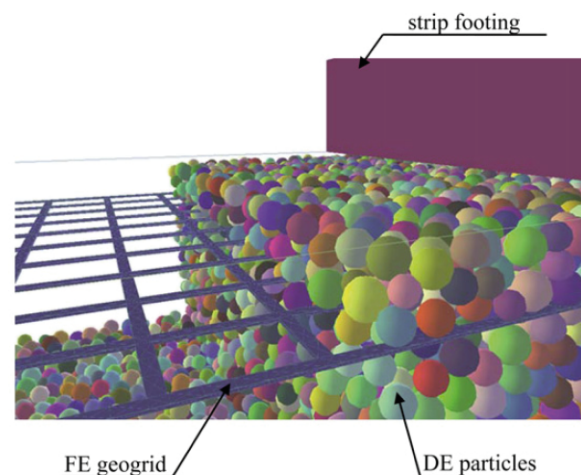


Figure 8. Coupled FE/DE strip footing [32].

Zhuang and Wang [33] compared the numerical response of a biaxial geogrid used in a piled embankment when modeled as an isotropic membrane, an orthotropic membrane, and a truss element. A parametric test was carried out on a hypothetical geogrid-reinforced embankment modeled in ABAQUS[®], without validation with experimental data. For the membrane models, a general 4-node quadrilateral membrane (designated M3D4) was used. The truss element model used a 2-node linear displacement element (designated T3D2). The three geogrid models were represented as linear-elastic materials. The results (Figure 9) showed a good agreement between the orthotropic model and the truss element model, while the isotropic model yielded a considerably higher tensile strength (33% difference). Moreover, in the four parametric tests (influence of embankment height, pile spacing, geogrid stiffness, and compression index of subsoil), the same trend was observed, where the isotropic model diverged from the orthotropic and truss element models (up to 65% difference).

In reference [34], the authors reported a 3D model to investigate the soil arching effect on pile-supported embankments reinforced with geogrids. The model consisted of eight-node brick elements to represent the soil particles with the EPPMC model, while the geogrid was represented by a membrane element on an elastoplastic regimen (no rigidity to flexion). The interface between the pile caps and surrounding filler/subsoil was taken as a surface-to-surface with tangential and normal coefficients. In the field data, the subsoil also contained water bags, and the authors reported a large number of attempts

to adjust the mechanical properties of the water bags (Figure 10) that were modeled with the same eight-node brick element as the soil particles. The model also considered the construction phases by adding filler in steps accordingly. The numerical model showed excellent correlation with the deformations and pressures observed in the field, across the initial load and after consolidation. The model was also able to capture the evolution of the arching shape (evaluating the stress distribution over time).

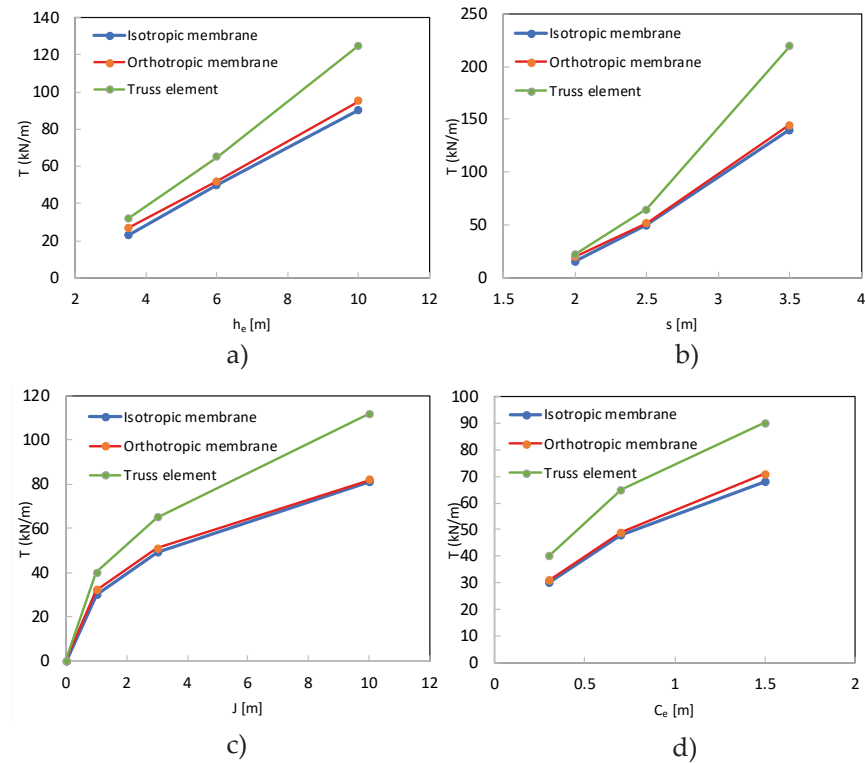


Figure 9. Comparison between isotropic, orthotropic, and truss element models: (a) effect of embankment height on the reinforcement stresses; (b) effect of pile spacing on the reinforcement stresses; (c) effect of geogrid stiffness; (d) effect of compression index of subsoil [33].

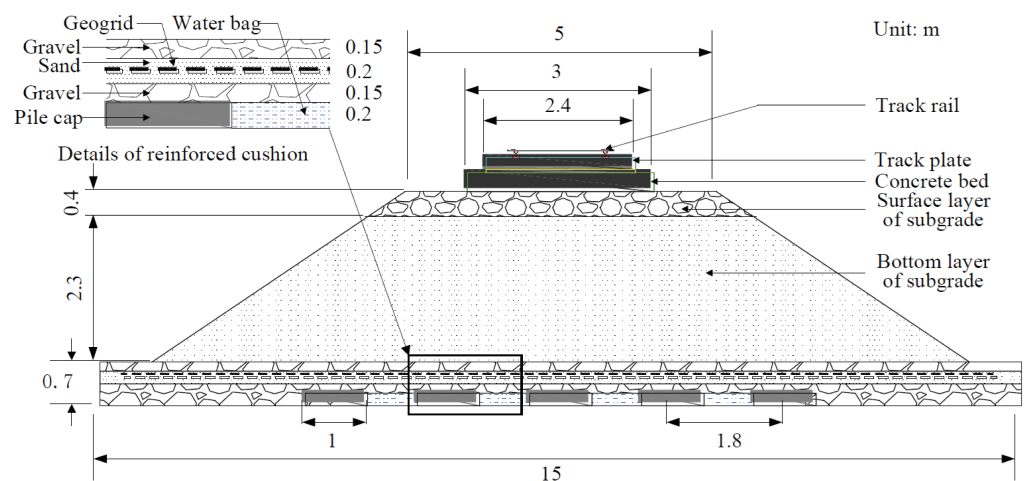


Figure 10. Cross-section of modeled embankment [34].

A comparison between using a continuous 2D sheet against the exact 3D geometry of a geogrid was presented in [15]. Geogrids have a complex geometry (Figure 11) that is frequently modeled using either a truss, bar, or cable components in 2D, and an equivalent plane sheet. This simplification was explored in their paper.

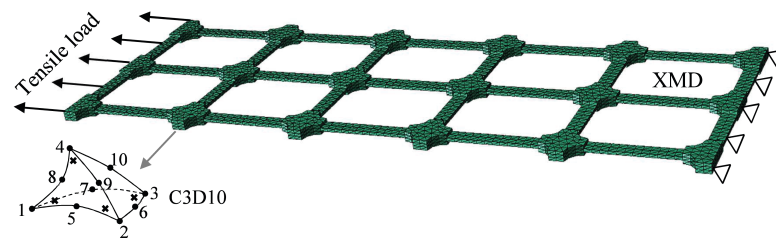


Figure 11. Geometry of the extruded geogrid used in 3D FEM models [15].

Although having easier to perform calculations, these geometry-simplified models come at a cost of extensive calibration to adjust the element stiffness through an equivalent thickness. The geogrid was modeled in ABAQUS[®] as a nonlinear elastoplastic with isotropic hardening to represent the different strength responses in the main directions of the geogrid. For the soil-confined model, the backfill was modeled by the EPPMC model. The soil–geogrid interaction was simulated with contact surface constraints (fully bonded master/slave contact) between the geogrid apertures and the granular soil filling the reinforcement, with no slippage allowed. A finite element comparison was made between hexahedral and tetrahedral formulations, and it was seen that the hexahedral elements provided a better correlation with experimental data. The study demonstrated that using the equivalent plane sheet without the proper calibration could lead to an underestimation in the design loads acting on the geogrid, coming from a stiffer response from the membrane/shell element type. Moreover, if simplifications are required (i.e., for the sake of lowering computation time in large models), then 3D models proved to be a good reference for estimating the equivalent sheet properties, in order to accurately represent the geogrid behavior. The exact geometry also proved appropriate to model the soil interaction, and the 3D model adjusted the experimental data reasonably well.

In reference [35], the authors utilized the three-dimensional particle flow code (PFC3D) to model single geogrid-encased stone columns under unconfined compression. The study employed the discrete element method (DEM) to investigate the effect of four factors (geogrid stiffness, column length, column diameter, and aggregate size) on the behavior of the columns. The study made use of experimental data to verify the numerical model, which aimed to carry out a parametric analysis. The constitutive models for geosynthetic and soil were determined by simulating tensile tests and flexural bending tests based on the ASTM standards. The soil–geosynthetic interaction was also considered in the model through the introduction of spherical balls with a high coefficient of friction and weak contact bonds. A laboratory test on a geogrid-encased stone column under unconfined compression, was treated as the baseline case for the parametric study. The results showed a good agreement between the numerical model and the corresponding laboratory test (vertical pressure and vertical strains).

Zhou et al. [36] compared 2D and 3D models in the analysis of reinforced piers. The study included several types of interfaces, as they represented a major factor in the performance of reinforced piers. The authors discussed the differences in the modeling considerations and the limitations of the 2D model. Only the 3D model could include the facing geometric properties of the concrete masonry units using a typical half-width offset, Figure 12. The reinforcement was modeled in the FLAC[®] package using the proprietary membrane elements for the 3D models and a “cable” element for the 2D model, given that the cable element did not provide bending resistance. The backfill was represented by the EPPMC model. The interfaces also used proprietary elements, i.e., linear-elastic springs with interaction coefficients obtained from the literature. The results indicated that different boundary conditions inherent to the model type (2D/3D) led to incomparable results. Lateral displacements at mid-height were about two times larger in the 2D model, while the peak volumetric strain on the reinforcement was 60% larger. The 2D model was conservative for peak displacements/stresses and presented different overall material responses, influenced by the necessary changes in boundary conditions in the 2D model.

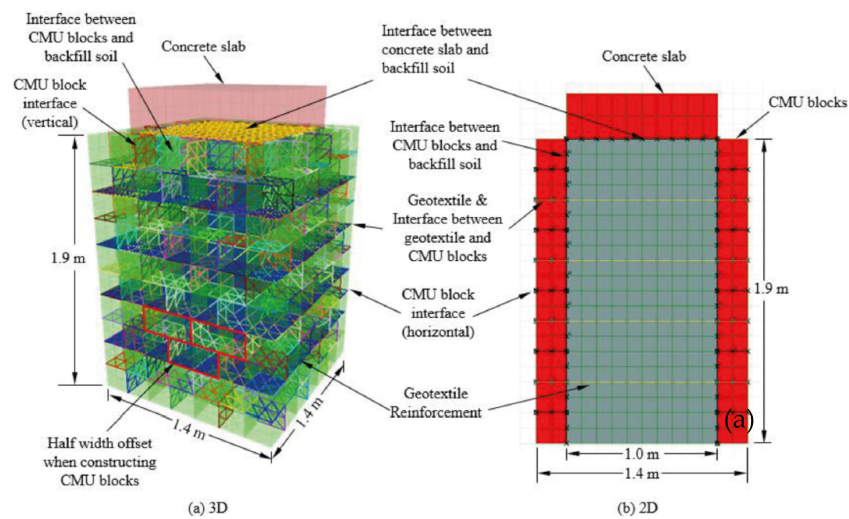


Figure 12. The 2D and 3D FEM geometry in [36].

Reference [37] described a three-dimensional modeling framework to simulate a biaxial geogrid under a pullout loading. The biaxial geogrid was modeled in ABAQUS[®] using an elastoplastic model with 8-node brick elements and the sand was represented by the EPPMC model with non-associated flow rule. The model consisted of a 5-part scheme illustrated in Figure 13. In the first step, the bottom soil domain (BS) was added in three stages, followed by the corresponding geostatic stresses in each stage. Then, the geogrid (GEO) and the soil at openings (Soil_{OPN}) were added in another step. The top-soil domain (TS) was then added in 15 steps. With this approach, the soil elements above and below the geogrid were allowed to directly interact with each other through the soil opening elements. To simulate the soil–geogrid interaction, a series of master–slave contacts were defined between the geogrid and the soil components. The horizontal soil-to-geogrid interface (GEO and TS/BS) was modeled as a hard Coulomb friction model; thus, no penetration between the soil and the geogrid was allowed during the pullout process. In the vertical soil-to-geogrid interface, separate friction definitions were made for the interface between the longitudinal and transversal ribs. In the longitudinal ribs, the vertical interfaces were assigned to a hard Coulomb contact (similar to that of the horizontal interface).

An investigation of the cyclic load behavior in pile-reinforced embankments was presented in [38]. The three-dimensional pile was modeled in ABAQUS[®] using 8-node brick elements (C3D8) for the embankment, soft soil, piles, and footing, and a 4-node membrane (M3D4) for the geosynthetic layers. To analyze the cyclic behavior, the granular soil that composed the embankment fill was modeled by a hypoplastic constitutive model. This model accounted for the influence of density and dilatancy (pyknosity), the pressure level (barotropy), and intergranular strain, requiring a total of 13 parameters. Since the model was not directly validated by experimental data, parameters from the hypoplastic model were retrieved from the literature (with some of them further calibrated by trial and error). The remaining elements followed a traditional linear-elastic formulation, with the soft soil represented by the CamClay model and the piles/geosynthetic modeled by an isotropic linear-elastic model. The soil–geogrid interface was simulated using the traditional surface-to-surface Coulomb friction model. The cyclic loading was modeled by a sinusoidal curve, simulating the cyclic loading of a vehicle wheel load. The parametric study featured a series of loading scenarios of traffic speeds (i.e., variations in amplitude and frequency of the cyclic loading). The hypoplastic model was able to accurately represent the embankment fill under static loading. Although no real data were made available for the cyclic loading scenarios, the numerical model indicated that the geosynthetic reinforcement reduced the soil arching effect and consequently decreased the cumulative settlement.

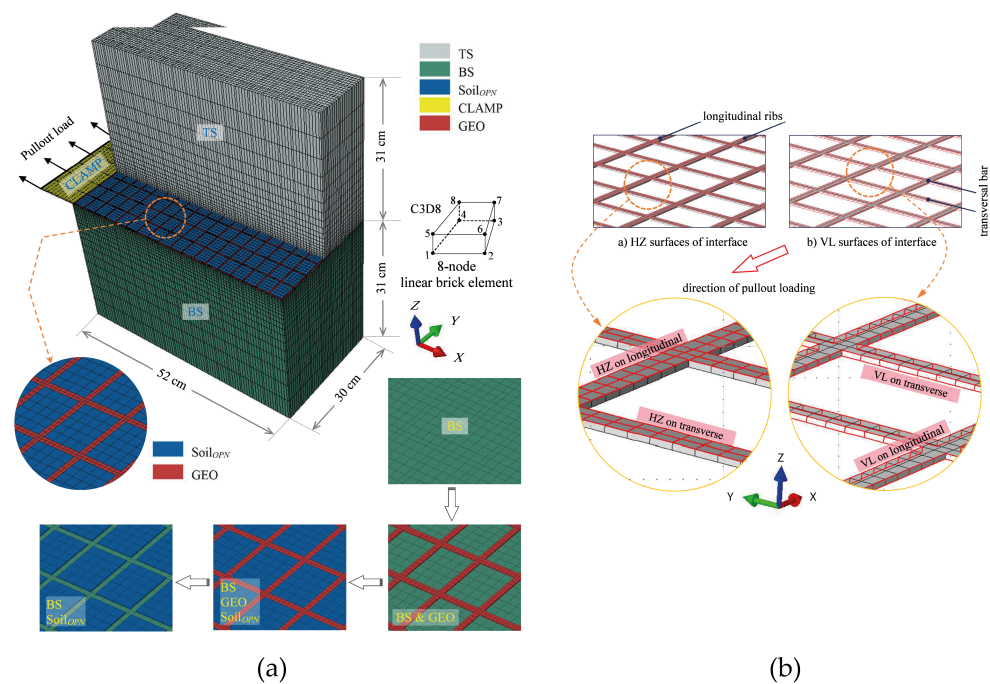


Figure 13. Details of the 3D mesh geometry for pullout modeling: (a) 5-part model, where BS and TS are the bottom and top soil domains, respectively; Soil_{OPN} is the soil between the geogrid openings; GEO is the geogrid and CLAMP is the non-deformable element that pulls the geogrid; (b) soil-geogrid contact interfaces [37].

In [39], a comprehensive series of 3D and equivalent 2D numerical analyses were performed focusing on the failure mechanisms of column-supported embankments (CSE), using FLAC3D[®]. The numerical analyses considered the failure height as the ULS stability metric, to make the models less computationally expensive. Eight scenarios included a base case and seven parametric variations using base case conditions, and the parameters for variation were center-to-center column spacing, column diameter, geosynthetic stiffness, and the clay's undrained shear strength. The scenarios were related to the base case by altering the column spacing, column diameter, geosynthetic stiffness, and the clay's undrained shear strength. The undrained-dissipated approach was used to calculate the two limiting conditions for a lateral spreading analysis, an undrained end-of-construction state, and a long-term state after dissipation of all excess pore water pressures, for investigating CSE failure modes. The method of excess pore water pressure dissipation and computed consolidation deformations were validated using a benchmark solution (one-dimensional consolidation and laterally drained consolidation comparison). Material parameters were calibrated such that the system response at the undrained end-of-construction and long-term dissipated conditions agreed with the instrumented case history data. The model was solved for equilibrium and an undrained end-of-construction state after the construction of every lift, and following undrained loading, pore water pressures were returned to the hydrostatic condition, and the model was solved for consolidation and a long-term dissipated state. The soil particles were modeled with traditional linear-elastic formulations and the geosynthetics were modeled as an orthotropic linear elastic material, allowing for mesh element removal when the given transverse strain reached the upper limit defined. The article concluded that, for the global stability analysis of CSEs, the conventional two-dimensional limit equilibrium method (LEM) is not appropriate. A comparison was made between the results of 2D limit equilibrium analyses and those of 3D numerical analyses. The comparison showed that 2D analyses resulted in unconservative factors of safety (FS) because they assumed failure by shear, whereas the columns of CSEs failed not by shear, but by bending and flexural tension. In addition, the 3D model indicated that the geogrid did not provide any resistance during failure, given that the failure was initiated after

the geogrid rupture, whereas the 2D analysis could not simulate the same effect order (geogrid was fully mobilized up until failure). The article also showed that the circular failure surface search in LEM would not be able to find the critical failure surface for CSEs, which involves the soil–structure interactions and failure within the foundation. This paper suggested that the LEM only correctly calculated the factor of safety when the failure surfaces were fully specified, and when both the geogrid and columns were excluded from the analysis. However, these conditions could not be met without the feedback output of a full 3D analysis.

Vibhoosha et al. [40] used ABAQUS[®] to evaluate the time-dependent performance of geocell-reinforced encased stone columns (GESC) using a time-dependent 3D stress–pore pressure coupled analysis. A key aspect of this work was to evaluate the influence of the geocell deformation on the response of GESC structures. The infill soil, stone column, embankment soil, and sand blanket used an EPPMC model. Lithomargic clay was modeled with the Modified Cam Clay (MCC) model, with properties calibrated through laboratory tests. The geogrid and geocell were modeled as isotropic linear elastic materials. The model featured the usual method of analyzing a singular column alongside its adjoining soil tributary zone. Leveraging the symmetry, only a quarter of the column and its associated region was simulated. Mesh dimensions were determined after multiple preliminary tests with varying element quantities. To ensure consistency and negate meshing errors, element dimensions were maintained as uniformly vertical. The preliminary time increment was set to 10^{-3} days. The lithomargic clay stratum and stone column utilized 20-node stress–pore pressure coupled brick elements with condensed integration (C3D20RP). The embankment substrate, geocell-sand mattress infill, and drainage overlay were constructed using 20-node quadratic brick elements with condensed integration (C3D20R). Lastly, the geogrid sheathing and geocell were depicted through eight-node membrane elements with minimized integration (M3D8R). Even with the use of reduced integration elements, the authors reported that the simulation had an average execution time of 7 h.

The material properties and the modeling approach were validated, aiming at replicating the load test results from the laboratory tests. The stress distribution in the geocell-sand mattress was uneven, peaking at the geocell pockets' mid-height and decreasing towards its edges. The tensile stress mobilized in the geocell pockets during embankment loading can differ, yet designs typically consider a constant tensile strength. The study further revealed that an increased geocell stiffness enhanced the weight transfer to stone columns and confined the infill material more effectively. This increased stiffness, attributed to the 3D structure of the geocells, resulted in a reduced ground surface settlement and improved weight transfer from the foundation soil to the encased stone column. The findings revealed that the stress concentration ratio (SCR) increased over time, stabilizing after consolidation, with an 85% improvement when a geocell layer was added to the geosynthetic encased stone columns (GESC). Importantly, the geocell-sand mattress reduced the vertical foundation soil settlement by 80% during embankment construction and decreased stone column bulging, especially when aggregates were chosen as the infill material. The numerical model developed in this study accurately represented the shape of the geocell and its relationship with the infill, addressing the shortcomings of the equivalent composite approach. The results suggested that GESC+GEOCELL configurations might offer a more cost-effective alternative to the commonly used geosynthetic reinforced piled embankment systems.

5. Conclusions

This study utilized a bibliometric analysis to map and understand the state of the art of GRS modeling. The bibliometric analysis proved to be a useful tool to capture research trends and relevant papers, taking into account a larger number of parameters and indicators. The various occurrence maps were used to quickly identify papers and authors that had the biggest impact within the field scope. The co-occurrence of keywords was a particularly useful tool to guide a more profound search in the database, highlighting

frequently combined words. The citation of documents map was also a reliable indicator for selecting documents with the highest impact. This approach proved to be faster, more comprehensive, and more reliable than traditional single metrics (e.g., citation number). The research trends in the field of GRS structures were analyzed using VOSviewer, and a co-occurrence map was used to identify the main related keywords for GRS modeling. The red cluster contained the keyword “Numerical Model”, which was also associated with terms such as “stiffness”, “experimental study”, “soil-structure interaction”, and “pullout test”. This cluster showed that numerical models are frequently used for studying GRS structures; however, three-dimensional models were less common and more recent. The finite difference method was also shown to be a common approach to modeling GRS structures. The “centrifuge” cluster highlighted the use of centrifuge models in the analysis of GRS structures. Centrifuge modeling is a technique used to simulate the full-scale behavior of soil structures by spinning a reduced-scale model to a higher gravitational field. The “embankment” and “retaining wall” clusters indicated the most common structures within the scope of the GRS papers analyzed in the present paper.

Soil-reinforced structures have become a trending topic in the past years. However, the design and numerical model still require further research. The following lessons can be summarized:

- Two-dimensional models are more common than three-dimensional, and although able to represent the overall structure behavior and predict peak stresses, they also require careful calibration with experimental data. Three-dimensional models are a more recent approach and generally produce better results, not only in terms of maximum stresses, but are also a better fit to the overall measured data.
- The FEM and DEM are both used to simulate the ultimate and serviceability states of geotechnical structures. The FEM is widely used to simulate the in-situ response of geosynthetics and has also been shown to perform well in the representation of soil behavior and soil-geosynthetic interactions. The DEM is also used for geotechnical modeling, being able to better represent the discontinuity of soil particles. In more recent approaches, a coupled analysis using both numerical techniques has shown great potential in leveraging the capabilities of each formulation (e.g., using the DEM to represent the soil and the FEM to represent the geosynthetics).
- The material properties and constitutive models have a high impact on the modeling and design of GRS. Experimental measurement of the in-situ response of both the reinforcement and the soil indicated that geotechnical structures are highly nonlinear, for both short-term and long-term responses. Thus, linear-elastic models usually did not fit lab or field measurement values, without requiring the cost of extensive calibration. Several papers showed that the isotropic linear-elastic assumption for geosynthetic materials leads to an overestimation of the tensile strength of the reinforcement.
- The use of isotropic models to represent geosynthetic materials tends to overestimate the peak stresses and strains acting on the reinforcement. Orthotropic models generally presented a better adjustment of measured data.
- Two recurring difficulties in GRS modeling are the boundary conditions and meshing. Full-scale GRS structures usually comprise many different materials, and often the disparity between measured results and simulation results was close to the boundary conditions (e.g., close to the toes in retaining wall models; extremities of piles in embankment models).
- The behavior of geosynthetics at small-scale laboratory conditions might not always represent large-scale field conditions. It is crucial to ensure that scale effects are appropriately accounted for in a model.
- If geosynthetics are involved in drainage or containment (like in the case of geomembranes or geonets), the numerical model should robustly handle hydraulic interactions. This includes considering factors like pore-water pressures and seepage forces.

- The definition of the soil–geosynthetic interface is an important factor in the overall response of a model. The synergy between the reinforcement and the soil increases mechanical performance and can also alter the rupture mode. Several studies showed the importance of direction-dependency in the consideration of interface elements. The efficiency of a geosynthetic in reinforcing soil is largely based on interaction parameters like friction and adhesion. Properly determining and incorporating these parameters is essential for accurate numerical modeling.
- Numerical models, regardless of their sophistication, are still approximations of real-world conditions. The actual ground conditions, presence of groundwater, varying loadings, and unforeseen soil properties can make field behavior diverge from model predictions. It is imperative that any numerical model used for geosynthetics be validated using field or laboratory data.
- In many real-world scenarios, geosynthetics do not work in isolation. They are part of a larger system that might include other reinforcements, drainage systems, and structural components. Ensuring the numerical model can integrate these systems effectively is essential.
- As design methodologies evolve, the use of 3D GRS models is encouraged and expected to become more prevalent. Three-dimensional models have been demonstrated to provide a more accurate representation of soil structures, both at the reinforcement level and the overall structure response under ULS/SLS conditions. At the reinforcement level, 3D models can better output the stress distributions within the geosynthetic, which could, for instance, be used to improve the geometry of geogrids and geocells. At the structure level, 3D models were able to capture complex load transfer mechanisms such as soil arching and the interaction between different structural components.

Author Contributions: L.P.: Data curation, Formal analysis, Funding acquisition, Investigation, Methodology, Writing—original draft, Writing—review and editing. M.P.-L.: Conceptualization, Data curation, Formal analysis, Funding acquisition, Investigation, Methodology, Project administration, Resources, Supervision, Writing—review and editing. R.V.: Conceptualization, Formal analysis, Funding acquisition, Investigation, Methodology, Resources, Supervision, Writing—review and editing. A.M.P.: Conceptualization, Data curation, Formal analysis, Funding acquisition, Investigation, Methodology, Resources, Supervision, Writing—review and editing. All authors have read and agreed to the published version of the manuscript.

Funding: The first author acknowledges financial support from the Portuguese Foundation of Science and Technology—FCT under the MIT Portugal PhD Grant PRT/BD/153383/2021. The financial support of FCT is also gratefully acknowledged through the projects UIDB/04450/2020 (RISCO), UIDB/00481/2020 (TEMA), UIDP/04450/2020 and CENTRO-01-0145-FEDER-022083 (CENTRO 2020).

Data Availability Statement: The original contributions presented in the study are included in the article, further inquiries can be directed to the corresponding authors.

Conflicts of Interest: The funders had no role in the design of the study; in the collection, analyses, or interpretation of data; in the writing of the manuscript; or in the decision to publish the results.

Abbreviations

The following abbreviations are used in this manuscript:

ADINA [®]	Automatic Dynamic Incremental Nonlinear Analysis
DEM	Discrete Element Method
EPPMC	Elastic perfectly-plastic Mohr-Coulomb model
FDM	Finite Difference Method
FEM	Finite Element Method
GESC	Geosynthetic-Encased Stone Columns
GRS	Geosynthetic-Reinforced Structures
FLAC [®]	Fast Lagrangian Analysis of Continua

MCC	Modified Cam Clay
ULS	Ultimate Limit State
SLS	Serviceability Limit State
YADE [©]	Yet Another Discrete Element

References

1. BS EN ISO 10318-1:2015; Part 1—Terms and Definitions. BSI Standards Limited: London, UK, 2015.
2. Allen, T.; Bathurst, R.; Berg, R. Global Level of Safety and Performance of Geosynthetic Walls: An Historical Perspective. *Geosynth. Int.* **2002**, *9*, 395–450. [[CrossRef](#)]
3. Vlček, J.; Drusa, M.; Gago, F.; Mihálik, J. Analysis of a Large-Scale Physical Model of Geosynthetic-Reinforced Piled Embankment and Analytical Design Methods. *Buildings* **2023**, *13*, 1464. [[CrossRef](#)]
4. Villard, P.; Huckert, A.; Briançon, L. Load transfer mechanisms in geotextile-reinforced embankments overlying voids: Numerical approach and design. *Geotext. Geomembr.* **2016**, *44*, 381–395. [[CrossRef](#)]
5. Augarde, C.E.; Lee, S.J.; Loukidis, D. Numerical modelling of large deformation problems in geotechnical engineering: A state-of-the-art review. *Soils Found.* **2021**, *61*, 1718–1735. [[CrossRef](#)]
6. Hatami, K.; Bathurst, R.J.; Di Pietro, P. Static Response of Reinforced Soil Retaining Walls with Nonuniform Reinforcement. *Int. J. Geomech.* **2001**, *1*, 477–506. [[CrossRef](#)]
7. Ho, S.; Rowe, R. Effect of wall geometry on the behaviour of reinforced soil walls. *Geotext. Geomembr.* **1996**, *14*, 521–541. [[CrossRef](#)]
8. Lopes, M.; Cardoso, A.; Yeo, K. Modelling performance of a sloped reinforced soil wall using creep function. *Geotext. Geomembr.* **1994**, *13*, 181–197. [[CrossRef](#)]
9. Karpurapu, R.; Bathurst, R.J. Behaviour of geosynthetic reinforced soil retaining walls using the finite element method. *Comput. Geotech.* **1995**, *17*, 279–299. [[CrossRef](#)]
10. Ling, H.; Cardany, C.; Sun, L.X.; Hashimoto, H. Finite Element Study of a Geosynthetic-Reinforced Soil Retaining Wall With Concrete-Block Facing. *Geosynth. Int.* **2000**, *7*, 163–188. [[CrossRef](#)]
11. Yun-min, C.; Wei-ping, C.; Ren-peng, C. An experimental investigation of soil arching within basal reinforced and unreinforced piled embankments. *Geotext. Geomembr.* **2008**, *26*, 164–174. [[CrossRef](#)]
12. Perkins, S. Constitutive modeling of geosynthetics. *Geotext. Geomembr.* **2000**, *18*, 273–292. [[CrossRef](#)]
13. BS EN ISO 10319:2015; Geosynthetics—Wide-Width Tensile Test. BSI Standards Limited: London, UK, 2015.
14. Walters, D.; Allen, T.; Bathurst, R. Conversion of Geosynthetic Strain to Load Using Reinforcement Stiffness. *Geosynth. Int.* **2002**, *9*, 483–523. [[CrossRef](#)]
15. Hussein, M.; Meguid, M. A three-dimensional finite element approach for modeling biaxial geogrid with application to geogrid-reinforced soils. *Geotext. Geomembr.* **2016**, *44*, 295–307. [[CrossRef](#)]
16. Leonardi, G.; Suraci, F. A 3D-FE Model for the Rutting Prediction in Geogrid Reinforced Flexible Pavements. *Sustainability* **2022**, *14*, 3695. [[CrossRef](#)]
17. Allen, T.; Bathurst, R. Combined Allowable Strength Reduction Factor for Geosynthetic Creep and Installation Damage. *Geosynth. Int.* **1996**, *3*, 407–439. [[CrossRef](#)]
18. Paula, A.M.; Pinho-Lopes, M.; Lopes, M.D.L. Combined effect of damage during installation and long-term mechanical behavior of geosynthetics. In Proceedings of the 4th European Geosynthetics Conference, Edinburgh, UK, 7–10 September 2008.
19. van Eck, N.J.; Waltman, L. Citation-based clustering of publications using CitNetExplorer and VOSviewer. *Scientometrics* **2017**, *111*, 1053–1070. [[CrossRef](#)] [[PubMed](#)]
20. Zupic, I.; Čater, T. Bibliometric Methods in Management and Organization. *Organ. Res. Methods* **2014**, *18*, 429–472. [[CrossRef](#)]
21. Börner, K.; Chen, C.; Boyack, K.W. Visualizing knowledge domains. *Annu. Rev. Inf. Sci. Technol.* **2003**, *37*, 179–255. [[CrossRef](#)]
22. Koerner, R.M.; Lord, A.E.; Hsuan, Y.H. Arrhenius modeling to predict geosynthetic degradation. *Geotext. Geomembr.* **1992**, *11*, 151–183. [[CrossRef](#)]
23. Zornberg, J.; Mitchell, J.; Sitar, N. Testing of Reinforced Slopes in a Geotechnical Centrifuge. *Geotech. Test. J.* **1997**, *20*, 470–480. [[CrossRef](#)]
24. Girout, R.; Blanc, M.; Dias, D.; Thorel, L. Numerical analysis of a geosynthetic-reinforced piled load transfer platform—Validation on centrifuge test. *Geotext. Geomembr.* **2014**, *42*, 525–539. [[CrossRef](#)]
25. Sia, A.; Dixon, N. Numerical modelling of landfill lining system—waste interaction: Implications of parameter variability. *Geosynth. Int.* **2012**, *19*, 393–408. [[CrossRef](#)]
26. Hatami, K.; Bathurst, R.J. Development and verification of a numerical model for the analysis of geosynthetic-reinforced soil segmental walls under working stress conditions. *Can. Geotech. J.* **2005**, *42*, 1066–1085. [[CrossRef](#)]
27. Huang, J.; Han, J.; Collin, J.G. Geogrid-Reinforced Pile-Supported Railway Embankments: A Three-Dimensional Numerical Analysis. *Transp. Res. Rec. J. Transp. Res. Board* **2005**, *1936*, 221–229. [[CrossRef](#)]
28. Saad, B.; Mitri, H.; Poorooshasb, H. 3D FE Analysis of Flexible Pavement with Geosynthetic Reinforcement. *J. Transp. Eng.* **2006**, *132*, 402–415. [[CrossRef](#)]
29. Le Hello, B.; Villard, P. Embankments reinforced by piles and geosynthetics—Numerical and experimental studies dealing with the transfer of load on the soil embankment. *Eng. Geol.* **2009**, *106*, 78–91. [[CrossRef](#)]

30. Yoo, C. Performance of Geosynthetic-Encased Stone Columns in Embankment Construction: Numerical Investigation. *J. Geotech. Geoenviron. Eng.* **2010**, *136*, 1148–1160. [[CrossRef](#)]
31. Rowe, R.K.; Liu, K.W. Three-dimensional finite element modelling of a full-scale geosynthetic-reinforced, pile-supported embankment. *Can. Geotech. J.* **2015**, *52*, 2041–2054. [[CrossRef](#)]
32. Tran, V.D.H.; Meguid, M.A.; Chouinard, L.E. Three-Dimensional Analysis of Geogrid-Reinforced Soil Using a Finite-Discrete Element Framework. *Int. J. Geomech.* **2015**, *15*, 04014066. [[CrossRef](#)]
33. Zhuang, Y.; Wang, K. Three-dimensional behavior of biaxial geogrid in a piled embankment: Numerical investigation. *Can. Geotech. J.* **2015**, *52*, 1629–1635. [[CrossRef](#)]
34. Zhou, W.H.; Lao, J.Y.; Huang, Y.; Chen, R. Three-dimensional Finite Element Modelling of Soil Arching in Pile-supported Geogrid-reinforced Embankments. *Procedia Eng.* **2016**, *143*, 607–614. [[CrossRef](#)]
35. Gu, M.; Han, J.; Zhao, M. Three-dimensional DEM analysis of single geogrid-encased stone columns under unconfined compression: A parametric study. *Acta Geotech.* **2017**, *12*, 559–572. [[CrossRef](#)]
36. Shen, P.; Han, J.; Zornberg, J.G.; Morsy, A.M.; Leshchinsky, D.; Tanyu, B.F.; Xu, C. Two and three-dimensional numerical analyses of geosynthetic-reinforced soil (GRS) piers. *Geotext. Geomembr.* **2019**, *47*, 352–368. [[CrossRef](#)]
37. Hussein, M.G.; Meguid, M.A. Improved understanding of geogrid response to pullout loading: Insights from three-dimensional finite-element analysis. *Can. Geotech. J.* **2020**, *57*, 277–293. [[CrossRef](#)]
38. Pham, H.V.; Dias, D.; Dudchenko, A. 3D modeling of geosynthetic-reinforced pile-supported embankment under cyclic loading. *Geosynth. Int.* **2020**, *27*, 157–169. [[CrossRef](#)]
39. Huang, Z.; Ziotopoulou, K.; Filz, G.M. 3D Numerical Analyses of Column-Supported Embankments: Failure Heights, Failure Modes, and Deformations. *J. Geotech. Geoenviron. Eng.* **2020**, *146*, 04020141. [[CrossRef](#)]
40. M P, V.; Bhasi, A.; Nayak, S. Three dimensional analyses of geocell reinforced encased stone column supported embankments on lithomargic clay. *Geomech. Geoengin.* **2022**, *18*, 458–476. [[CrossRef](#)]

Disclaimer/Publisher’s Note: The statements, opinions and data contained in all publications are solely those of the individual author(s) and contributor(s) and not of MDPI and/or the editor(s). MDPI and/or the editor(s) disclaim responsibility for any injury to people or property resulting from any ideas, methods, instructions or products referred to in the content.